Metabolite yields of CMB and combined method revealed significant variations (p<0,05) for lactate, N-acetylated metabolites and inositol(scyllo and myo).
As already known degradation of ethanolamine plasmalogens were observed within the lipophilic extracts after PCA extraction.
All methods were reproducible, whereas the CMB method variations were smallest.

Table 1: Summary of metabolite yields in µmol·g wet weight (mean ± standard deviation) from PCA, CMB and combined method.

Metabolites	PCA extraction (n = 4)	CMB method (n = 3)	Combined technique (n = 3)	p-Values PCA vs combined method	p-Values CMB vs combined method
Lactate	123,5 ± 11,0	129,4 ± 3,6	138,4 ± 4,4	**0,0413**	**0,0265**
Alanine	11,5 ± 0,9	11,7 ± 0,6	12,2 ± 0,7	0,1448	0,2021
N-Acetyl CH_3	59,6 ± 5,1	62,0 ± 1,3	65,4 ± 2,3	0,0649	**0,0446**
Glutamine	73,0 ± 6,1	73,5 ± 2,3	77,3 ± 3,6	0,1653	0,0995
GABA	21,0 ± 1,8	21,5 ± 0,3	22,5 ± 0,8	0,1267	0,0515
Glutamate	62,5 ± 5,5	66,2 ± 0,8	68,9 ± 3,4	0,0701	0,1322
Succinate	7,5 ± 0,6	6,9 ± 0,8	7,7 ± 0,5	0,3305	0,0733
Aspartic acid	12,8 ± 1,2	14,4 ± 0,4	14,8 ± 1,0	**0,0340**	0,2797
Inositol(scyllo)	5,6 ± 0,5	13,6 ± 1,3	8,6 ± 0,8	**0,0029**	**0,0210**
Taurine	6,2 ± 0,4	7,1 ± 0,3	6,8 ± 0,6	0,1083	0,2196
Creatine	63,1 ± 4,9	66,7 ± 2,5	67,9 ± 6,8	0,1600	0,3127
Inositol (myo)	89,7 ± 6,7	91,8 ± 3,4	99,2 ± 2,0	**0,0342**	**0,0155**
N-Acetyl-aspartate	57,9 ± 5,2	61,2 ± 4,8	67,5 ± 4,0	**0,0234**	0,0795
totalCholine	20,3 ± 1,7	20,2 ± 0,5	20,8 ± 1,5	0,3674	0,2966

Conclusion: The new combined method ensures an inactivation of all enzymes due to protein precipitation in a second extraction step, which prevents e.g. erroneous amino acid concentrations. Coprecipitation of metabolites was not observed. Therefore, it is a suitable technique to extract hydrophilic and lipophilic compounds simultaneously.

References:

[1] Le Belle,J.E. et al.(2003), *NMR in Biomed.*,15,37-44.
[2] Katyal,S.L. et al.(1985), *Lipids*, 20(3),201-203.

654

Classification of oligodendroglial tumours and GBM using 1H HR-MAS metabolic profiles

R. Ferrer-Luna[1], J. Calvar[2], J. Morales[3], H. Martinetto[2], M. Martinez-Bisbal[4], M. Cerdá-Nicolás[5], G. Sevlever[2], D. Monleón[6], **B. Celda**[7];
[1]Physical-Chemistry, Universitat de Valencia, Burjassot (Valencia), Spain, [2]FLENI, Buenos Aires, Argentina, [3]UCIM, Universitat de Valencia, Valencia, Spain, [4]CIBER-BBN. ISC-III. Universitat de Valencia, Burjassot (Valencia), Spain, [5]Pathology, Universitat de Valencia, Valencia, Spain, [6]Research Foundation. HCUV, Valencia, Spain, [7]Physical-Chemistry, CIBER-BBN. ISC-III. Universitat de Valencia, Burjassot (Valencia), Spain.

Introduction: GBM are the most aggressive brain tumour type, however low grade Oligodendroglial Tumours (OT) are more indolent, with slow growth and tend to be chemosensitive[1]. Anaplastic features in OT could be controversial in tumour grading, making difficult obtain unambiguous prognostic factor. New support tools for a better prognostic and patient treatment in histopathological borderline or ambiguous tumours can clinically helpful. The purpose was determining whether ex vivo metabolic profiles by HR-MAS, using eTUMOR protocols[2,3], distinguish between classes of glial tumours: low grade Oligodendroglial Tumours vs high grade GBM.

Materials and Methods: Metabolic profiles of 20 OT and 30 GBM were obtained. Spectra were acquired at 600MHz and 4ºC. CPMG sequence was used as T2_filter and monodimensional spectra were processed. In order to assess tumour tissue type and amount: cellularity, necrosis, and infiltrate normal brain, biopsies were histopathology analyzed after HR-MAS experiments. Aliphatic and Aromatic regions were normalized to total spectra area. Spectra were binned into 0.01 ppm buckets to reduce the impact of misalignment, 37 metabolites corresponding with 129 resonances previously assigned[4,5] were evaluated by Unsupervised analysis (PCA and Hierachical_Clustering). A supervised learning approach was used to build a two class prediction model based on their histopathological class (OT_vs_GBM) and grade (II_vs_III). We performed an evaluation of DLDA algorithm and 6 different prediction model were built with 2, 5, 10, 20, 35, 40 resonances. The training error of this prediction models were determined using Leave_One_Out_cross_validation. The performance of classification rule was validated with 8 independent GBM, and OT not used in the feature selection process.
Results and Conclusion: Figures 1 and 2 show average binned Spectra and PCA for GBM and OT. Among the 10 most discriminant assigned resonances contributing to the classifier, Myoinositol, Creatine, Valine, Isoleucine, Choline, GABA, Alanine were found. Error rate in train set was 0.06. The application of this clasification rule based on 40 resonances to an independent test set, yielded an error rate of 0/4 for OT , 0/4 for GBM. Many metabolites statistically significant have been previously associated with increased hypoxia[6]. These results show that pattern recognition approach from metabolic profiles can support glial tumour classification.

References:

1- Cairncross G. et al.(1998). *J.National Cancer Institute;90,19.*
2- Celda B., et al.(2006). *Adv.Exp.Med.Biol.*;587:285-302.
3- www.etumour.net
4- Govindaraju V., et al.(2000); *NMR in Biomedicine*;13:129-153.
5- Martinez-Bisbal MC., et al.(2004); *NMR in Biomedicine*;17:191-205.
6- Erb G., et al.(2008). *Mag Res. In Medicine*;59;959-965.

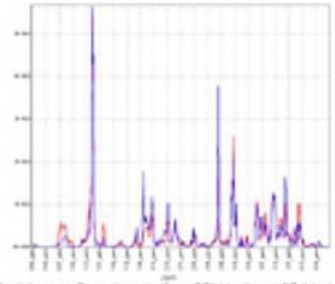

Fig.1 Average Binned spectra from GBM (red) and OT (blue).

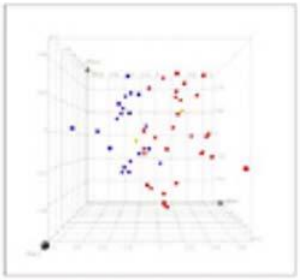

Fig.2 Scatter plot of Principal Component Analysis

655

Tissue typing within glial tumours

A. Croitor Sava[1], M. C. Martinez-Bisbal[2,3], B. Celda[2,3], J. Cerda[4], S. Van Huffel[1];
[1]Dept. of Electrical Engineering (ESAT-SCD), Katholieke Universiteit Leuven, Leuven, Belgium, [2]Departamento de Quimica-Fisica, Facultad de Quimica, Universitat de Valencia, Valencia, Spain, [3]CIBER-BBN, ISC-III, Universitat de Valencia, Valencia, Spain, [4]Departamento de Patología, Facultad de Medicina, Universitat de Valencia, Valencia, Spain.

Introduction and Purpose: Heterogeneity is a routinely observed characteristic of glial tumors and this affects not only the tumor grading but also the

tissue typing within the tumor region. Histopathological evaluation of tumor tissue specimens allows us to distinguish three basic tissue classes: necrotic tissue, high cellularity tumor tissue or border tumor tissue. The purpose of this study is to obtain the same separation between above mentioned tissue classes using information coming from high-resolution magic angle spinning technique (HR-MAS). To this aim we investigate the metabolic profile of different grades of glioma spectra.

Materials and Methods: 1D PRESAT HR-MAS data were acquired on 52 patients (27 glioblastoma, GBM, 7 grade III glioma and 18 grade II glioma) at 11.7 T (500 and 600 MHz for H) at 0-4 ^{0}C and 4,000 Hz spinning rate (eTUMOUR protocols [1]) using BRUKER-Analytik-GmbH spectrometers. The spectra were preprocessed as described in [2]. The concentration of NAA, Cr, Cho, PCho and lipids (Lip1 at 0.9ppm and Lip2 at1.3ppm) are estimated and the metabolites ratios with respect to Cr are computed.

Results: A clear separation among the three tissue classes is obtained using clustering analysis, see Figure 1. The variability in concentration of the selected metabolites is directly related with the considered tissue types. The metabolic ratios present a high statistical sensitivity in detecting these classes regardless the grade of the tumor, see Table1. For necrotic tissue Lip(s)/Cr ratio values are very high in comparison with Cho(s)/Cr values, while Naa/Cr remains low. High cellularity tissue is characterized by high Cho/Cr values. Also the Lip/Cr values stay high but are much lower in comparison with the values within necrotic region. Naa/Cr is very low. For border tissue we noticed a considerable increase in the value of Naa/Cr compared to the other tissue types.

Conclusions: Our results suggest a strong correlation between tissue type and the metabolic profiles in glial tumors. A clear separation between necrotic, high cellularity and border tumor tissue is obtained regardless the tumor grade. This can represent a critical step for posterior metabolic subtype classification and could be used for a more appropriated definition of tissue types in obtaining nosological images [3].

References:

[1] http: // www.etumour.net
[2] Poullet J.B et al (2008), *Proc. EMBC 2007*: 180066.
[3] Croitor Sava A., et al (2008), Proc *MBEC 2008:340-343*

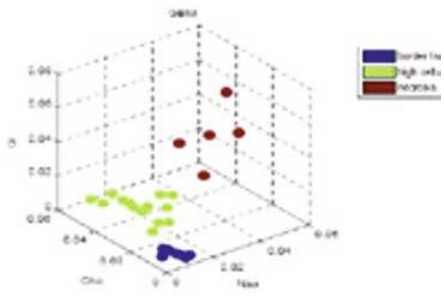

Figure 1 Clusters within GMB tumor group plotted in the space described by Cr, Cho and Naa

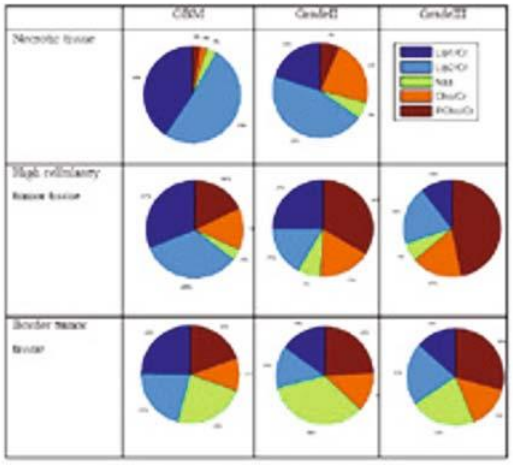

Table 1 Metabolic ratios for different tissue types detected within the available glial tumor groups

656

Automatic detection of amyloid plaques on ex vivo APP/PS1 mice using a zoom T2-weighted spin echo sequence

B. Marty, J. Flament, C. Giraudeau, S. Ahmed Ghaly, F. Lethimonnier, F. Boumezbeur, J. Valette, S. Mériaux;
Neurospin, CEA/DSV/I2BM/Neurospin, Gif-Sur-Yvette, France.

Purpose/Introduction: Amyloid plaques are a marker of Alzheimer's disease which are traditionally detected on T2* images taking advantage of the susceptibility effect due to iron embedded inside them. However it has been recently reported that T2 contrast might be more efficient to detect cortical plaques [1]. In this context, the goal of the present study was to compare two different strategies: (i) a conventional T2* gradient echo sequence with volume coil [2], and (ii) a zoom adiabatic T2 spin echo sequence with surface coil similar to ref.[1]. The images acquired in the APP/PS1 mouse brain ex vivo using the two approaches were compared based on their ability to allow successful plaques detection using a home-made automatic procedure.

Subjects and Methods: A transgenic APP/PS1 mouse was sacrificed and its brain was immersed in a solution containing formalin and GdDOTA (DOTAREM, Guerbet) according to a protocol previously established [2]. Experiments were performed on a 7T small animal MRI scanner (Bruker). T2-weighted images were obtained with a 3D adiabatic zoom multi-SE sequence (Fig.1) (TR/TE=500/40ms, resolution=50µm3, Tacq=10h) using a home-made quadrature surface coil. For comparison, T2*-weighted images were acquired using a 3D multi-GE sequence (TR/TE=1000/16ms, resolution=60x60x120µm3, Tacq=11h30). An automatic procedure based on local intensity gradients written in Matlab was used to segment amyloid plaques.

Results: Thanks to the high resolution zoom sequence combined to the increased sensitivity of surface coil, the T2 strategy allows resolving individual plaques ex vivo (Fig. 2a and 3a) in a reasonable time, including in deep regions of the brain far from the coil. On T2* images, cortical blood vessels appear as hypointense signal and can disturb the detection of amyloid plaques in this area (Fig. 2b and 3b). This might explain why the segmentation algorithm fails to selectively detect plaques on T2* images, while it seems to work well on T2 images (Fig.3).

Discussion/Conclusion: In this study, we have shown that we are able to automatically localize individual plaques ex vivo on APP/PS1 mice combining the zoom spin echo sequence and our segmentation procedure. An histologi-